

Supplementary information for:

Sr- and Mn-doped LaAlO_{3-δ} for Solar Thermochemical H₂ and CO Production

Anthony H. McDaniel,^{*a} Elizabeth C. Miller,^{§a,b} Darwin Arifin,^{‡a} Andrea Ambrosini,^b Eric N. Coker,^b Ryan O'Hayre,^c William C. Chueh,^{||a} and Jianhua Tong^{*c}
Synthesis:

Powders were synthesized using a modified Pechini method. Stoichiometric amounts of nitrate precursors, M^x(NO₃)_x•yH₂O, were dissolved in DI water. In a separate beaker, ethylenediaminetetraacetic acid (EDTA) was dissolved in ammonium hydroxide. The solutions were combined with stirring, citric acid was added, and the pH was adjusted as necessary with additional ammonium hydroxide until the solution was transparent, and no precipitates were present. The solution was heated with stirring until a viscous gel formed. The gel was heated in a furnace or drying oven at 250 °C until a black resin formed. The resulting ash was collected, ground with a mortar and pestle and calcined at 800 °C for 6 h to burn off any remaining organics or nitrates. Powdered samples used in the kinetic analysis were further calcined at 1350 °C for 24 h. Pellets used in the thermogravimetric analysis (TGA) and XRD analysis were made by adding polyvinyl butyral (PVB) binder to the powder (2 wt% equivalent) and then grinding the mixture with acetone using a mortar and pestle until dry and well-mixed. 0.6 – 0.8 g of this resultant mixture was uniaxially dry-pressed into pellets using a 13 mm die. The pellets were fired at 1350 °C for 24 h with a heating and cooling ramp rate of 3 °C/min to achieve the final pellet.

Characterization:

Room temperature x-ray diffraction (XRD) was performed on the sintered pellets using a Bruker D8 Advance diffractometer in Bragg-Brentano geometry with Cu K α radiation and analyzed with JADE 7.0+ analysis software to identify crystallographic phases present.¹ The XRD figure below (figure S1) shows the three perovskite materials adopt the rhombohedral LaAlO₃ structure (R-3c, PDF #01-070-4111). TGA was performed on a TA Instruments SDT Q600 under thermally reducing (Ar) and carbon dioxide splitting (CO₂) conditions. Argon and CO₂ gas streams both passed through getters to remove traces of oxygen prior to entering the TGA. Samples for TGA analyses were sintered bars of material (approx. 1.7 x 6 x 1 mm) placed atop a Pt crucible. Thermochemical cycling experiments in the TGA were conducted under heating and cooling rates of 15 °C/min and gas flow rates of 100 ml/min. The sample was reduced at 1350 °C under Ar. After dwelling for 60 minutes, the sample was ramped down to 1100 °C where the gas was switched to CO₂. After a 60 minute dwell period, the sample was ramped down to 850 °C, and held again for 60 minutes before cooling to room temperature. Weight loss during reduction implied oxygen loss, while weight gain under CO₂ implied reoxidation of the sample via splitting of CO₂. (figure S2) Post-TGA, the bars were ground into

powder and examined using XRD to determine if phase changes had occurred; the materials maintained the perovskite structure.

¹ Jade+, 9.1; Materials Data Inc., Livermore, CA, 2009.

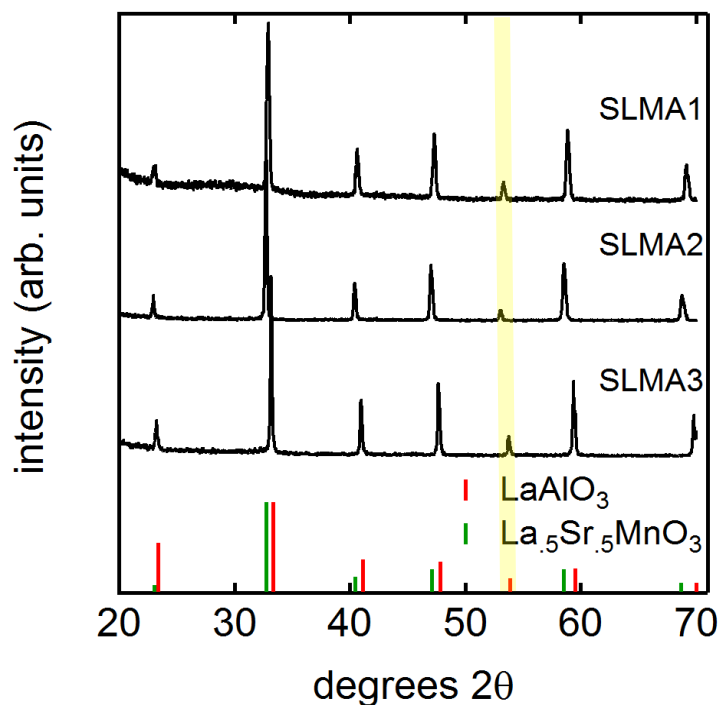


Figure S1: Powder XRD of SLMA compounds and reference peaks corresponding to the rhombohedral LaAlO₃ and La_{0.5}Sr_{0.5}MnO₃ perovskite phases. The SLMA perovskites clearly adopt the rhombohedral phase, as highlighted by the peak at approximately 54 °2θ (yellow band).

Kinetic Measurements:

The perovskites and commercial ceria powders were reduced and oxidized in a stagnation flow reactor (SFR) equipped with a modulated effusive beam mass spectrometer and laser-based sample heater. Salient features of the experimental apparatus consist of a stainless-steel gas-handling manifold, ceramic reactor core, high-temperature furnace, and 500 W near-IR laser. In stagnation flow, the gas-phase region above the sample between centerline and reactor wall can be considered an ideal one-dimensional stagnation plane governed by diffusive transport. This is an important attribute that distinguishes the fluid dynamics of this reactor type from others typically used to characterize kinetic behavior of ferrites and other materials used in thermochemical cycles, namely, packed bed reactors, flow tube reactors, and flow geometries common to thermogravimetric analyzers. Approximately 100 mg of powder were placed in a loosely-packed shallow bed within the stagnation plane allowing gases to access all exposed

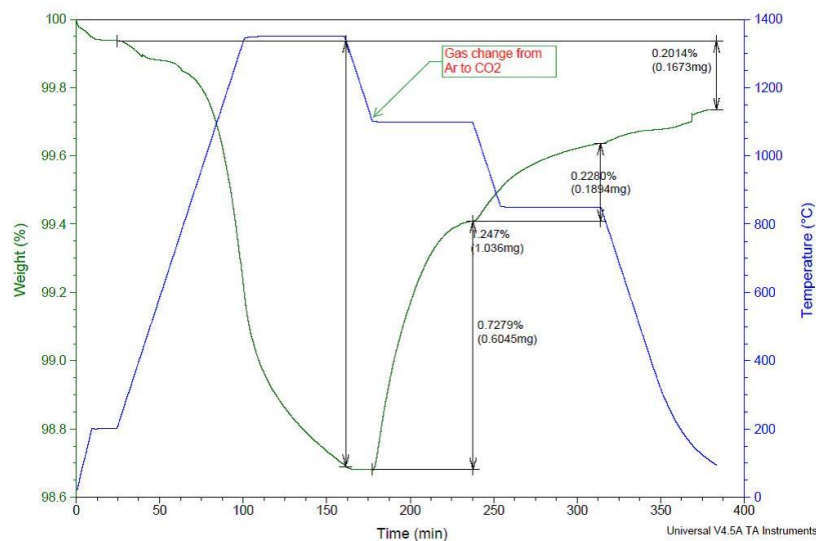


Figure S2: Representative TGA of SLMA3 showing the weight loss upon reduction under Ar and subsequent weight gain upon the introduction of CO₂ at 1100 °C and 850 °C.

surfaces within a well-mixed control volume. Gas compositions exiting the flow reactor were measured using a differentially pumped, modulated effusive beam mass spectrometer.

Thermal reduction (TR) was accomplished by heating the perovskite or ceria to 1350 – 1500 °C in a helium flow (500 sccm) until the desired extent of reduction was achieved. Water

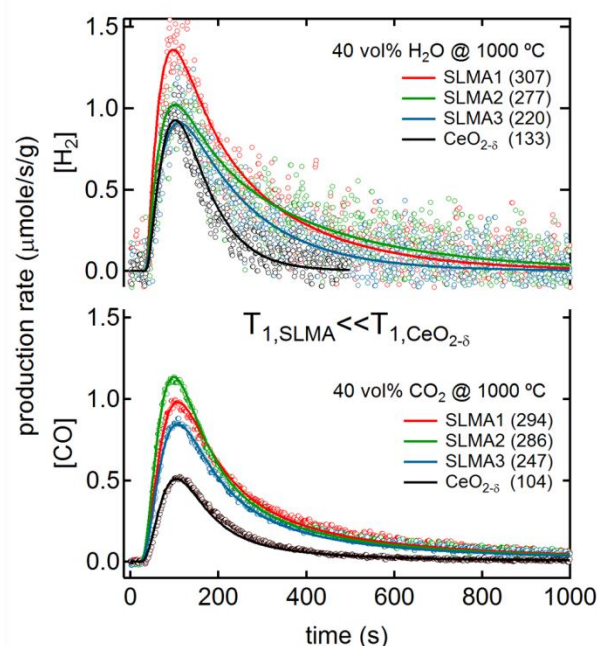


Figure S3: (top) H₂ and (bottom) CO production rates as a function of time measured during oxidation in 40 vol% H₂O or CO₂ at 1000 °C (open symbols). SLMA1-3 thermally reduced at 1350 °C in He. CeO₂ thermally reduced at 1500 °C in He. The total amount of H₂ or CO produced in μmoles/g material is shown in parentheses. Solid lines are the results of kinetic modelling.

splitting (WS) and carbon dioxide splitting (CDS) were performed using 40 vol% steam or carbon dioxide in He with a total flow rate of 500 sccm for a specified time interval at 1000 °C. The total reactor pressure for both TR and WS or CDS was 75 Torr. Shown in figure S3 are the H₂ and CO production rates for SLMA1-3 and CeO₂, measured during WS and CDS over previously reduced oxides. Nearly 3× more H₂ and CO are produced by the SLMA compounds when reduced at 1350 °C, as compared to CeO₂ reduced at 1500 °C which is a more conventional reduction temperature for CeO₂. Both materials were oxidized at 1000 °C.

Numerical Methods:

A numerical approach to analyzing the transient H₂ and CO production rates observed during WS and CDS was devised that accounts for: 1) kinetic processes occurring in the solid state; 2) the finite time required to introduce water vapour into the reacting volume; 3) detector time lag; and 4) dispersion/mixing of the H₂ evolved from the solid as it is transported downstream of the reactor volume to the detector. Impacts of the aforementioned experimental artifacts (namely 2 – 4 listed above) are not fully addressed by researchers in this field of science even though they can lead to erroneous conclusions regarding both the nature of rate limiting processes and the energetics associated with them. As shown in figure S4 panel (a), steam is introduced into the reactor volume by way of a step-function input that initiates the solid-state chemistry. We determined the shape of this step-function using a transient, 3-D computational fluid dynamics model of our reactor inlet under various operating conditions (note the minimal dispersion and narrow temporal width of the step). We have also measured similarly rapid gas injection behavior in tracer studies used to determine the space velocity and number of ideal CSTR reactor volumes in the dispersion model. The ensuing chemistry is treated like a black-box that is functionally described by various kinetic models taken from solid-state kinetic theory (panel (b) in figure S4), which track a single variable (α) representing the extent of reaction (i.e., the rate of progress). The output of the black-box is a waveform that describes the temporal evolution of H₂ resulting from the oxidation chemistry and serves as the input molar flow rate to the first in a series of ideal, continuously-stirred tank reactors (CSTR). The example given here is for model F2, which is a second order relation of the form: $f(\alpha) = (1-\alpha)^2$. Conceptually, the solid-state kinetic model produces a transient pulse-like input of H₂ into the CSTRs that is then stretched in time due to the physical actions of dispersion and mixing (panel (c) in figure S4). Governing kinetic behavior and the associated energetics are deduced by least-squares fitting the experimental H₂ production rate waveforms to simulations based on sampling various solid-state kinetic models.

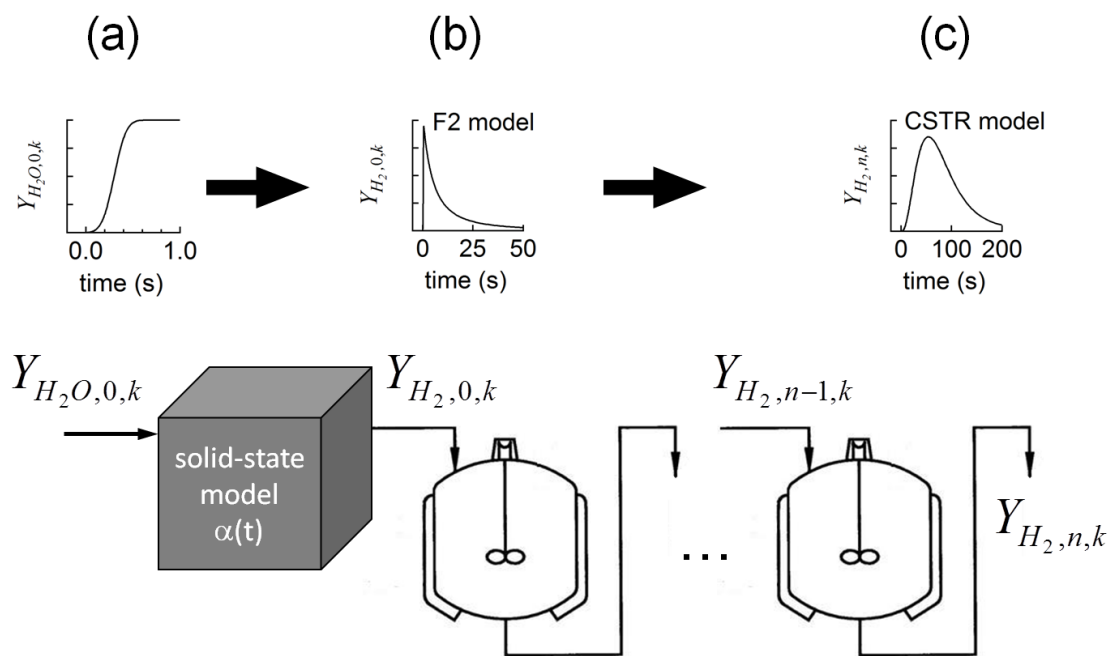


Figure S4. Representation of kinetic model used to describe hydrogen production via the WS process.